

**REVIEW ARTICLE**ISSN:2394-2371
CODEN (USA):IJPTIL**FTIR –ATR : A BREIF REVIEW**

Pooja Yadav*, Priyanka Maurya

Department of Pharmaceutics, Pranveer Singh Institute of Technology, Kalpi Road, Bhauti, Kanpur, U.P., India

ABSTRACT

FTIR was presented by German born American physician Albert Michelson in 1887. Here in this article it is described about design, instrumentation, sampling techniques and application of FTIR – ATR. Penetrating into basics of molecular vibrations might help us to understand whether, when and how complementary information obtained by micro FT-IR could become useful in our research and/or diagnostic activities. This review is aimed at illustrating some principles of Fourier transform (FT) IR spectroscopy and attenuated total reflectance (ATR). The IR region of the electromagnetic spectrum has dimension of wave numbers extending from ~13000 cm⁻¹ to ~10 cm⁻¹, with near-IR, mid-IR, and far-IR regions spanning from ~13000 cm⁻¹ to 4000 cm⁻¹, from 4000 cm⁻¹ to 400 cm⁻¹, and from 400 cm⁻¹ to 10 cm⁻¹ wave numbers, respectively. In pharmaceutical industry, IR spectroscopy has gained the popularity not only in the ease and expeditiousness of the samples measured but also in the quality of results obtained. We have also enlisted the Issues surrounding traditional transmission sample preparation . IR spectral data and applicative examples. The mid-IR absorbance spectrum is one of the most information-rich and concise way to represent the whole “omics” of a cell and, as such, fits all the characteristics for the development of a clinically useful biomarker. Also by understanding the molecular vibrations will greatly help us in our research and diagnostic activities. Likewise technique of ATR has also proved to be a wonder for researchers and spectroscopists around the world.

Keywords: - FTIR , ATR, transfectance,vibrational spectroscopy.**INTRODUCTION**

FTIR: FTIR spectroscopy is a vibrational spectroscopic technique that can be used to optically probe the molecular changes associated with diseased tissues [1-3]. The method is

employed to find more conservative ways of analysis to measure characteristics within tumor tissue and cells that would allow accurate and precise assignment of the functional groups, bonding types, and molecular conformations. Spectral bands in vibrational spectra are molecule specific and provide direct information about the biochemical composition. FTIR peaks are

Corresponding Author:*Pooja Yadav**Dept. of Pharmaceutics,
Pranveer Singh Institute of Technology,
Kalpi Road, Bhauti, Kanpur, U.P. IndiaE.Mail: coolpoojayadav93@gmail.com

Article Published: Oct.-Dec. 2016

relatively narrow and in many cases can be associated with the vibration of a particular chemical bond (or a single functional group) in the molecule [4,5]. Conventional spectroscopy is frequency domain spectroscopy in which radiant power data are recorded as function of frequency. In time domain spectroscopy, which is achieved by Fourier Transform (FT), radiant power data is recorded as a function of time. In previous case, radiant power (v) is plotted against frequency (ν) (Hz) while in later, against the time [6]. Michelson interferometer (MI) changes the frequency of electro magnetic radiation (EMR) from source to proportionately slower oscillating signal. The sum of slower oscillating signal is carried to the computer which mathematically separates the signal into individual oscillations and calculate the oscillations of corresponding frequencies of observed radiation. This data is continuously recorded. The amplitude of each resolved oscillations is a function of intensity of radiation. A mathematical method called Fourier Transform (FT) is used to convert time domain spectrum to conventional frequency domain spectrum.[7]

In pharmaceutical industry, IR spectroscopy has gained the popularity not only in the ease and expeditiousness of the samples measured but also in the quality of results obtained .[8] The pharmaceutical quality control of active pharmaceutical ingredients (API) includes (i) the

qualitative analysis for the identification of raw materials, intermediate, and finished products as well as for the evaluation of the ability of API to occur in different crystalline forms, known as polymorphism; (ii) the quantitative analysis of API in several pharmaceutical dosage forms; and (iii) monitoring the stages in pharmaceutical products development such as homogenization of API in the mixture, drying, packaging, etc. [9,10]

ATR: The technique of Attenuated Total Reflectance (ATR) has in recent years revolutionized solid and liquid sample analyses because it combats the most challenging aspects of infrared analyses, namely sample preparation and spectral reproducibility

Issues surrounding traditional transmission sample preparation :

The two most common forms of sample preparation for solids both involve grinding the material to a fine powder and dispersing it in a matrix. The ground material can be dispersed in a liquid to form a mull. The most commonly used liquid is mineral oil (nujol). Typically no more than 20 mg of solid is ground and then one or two drops of nujol are used to create a paste which is then spread between two Mid-Infrared transparent windows e.g. NaCl, KBr, CaF₂. The sample is now ready to be placed in the spectrometer for analysis by transmission.

Overall, sample preparation is easier for liquid transmission studies when compared to solid transmission sampling but both suffer from inevitable reproducibility issues given the complexity of the sample preparation methods. In addition, preparation can be very messy and time consuming and is further complicated by difficulties in getting sample to matrix ratios correct and homogenous throughout the sample. The materials involved are fragile and hygroscopic and the quality of measurements can be adversely affected if handled or stored incorrectly. The technique of Attenuated Total Reflectance addresses these issues.

PRINCIPALS OF ATR

An attenuated total reflection accessory operates by measuring the changes that occur in a totally internally reflected infrared beam when the beam comes into contact with a sample (indicated in Figure 4). An infrared beam is directed onto an optically dense crystal with a high refractive index at a certain angle. This internal reflectance creates an evanescent wave that extends beyond the surface of the crystal into the sample held in contact with the crystal. It can be easier to think of this evanescent wave as a bubble of infrared that sits on the surface of the crystal. This evanescent wave protrudes only a few microns ($0.5 \mu - 5 \mu$) beyond the crystal surface and into the sample. Consequently, there must be good contact between the sample and the crystal

surface. In regions of the infrared spectrum where the sample absorbs energy, the evanescent wave will be attenuated or altered.[11]

INSTRUMENTATION OF ATR

Most atr units are designed as horizontal crystals with a type of clamping utility that ensures good sample contact for solids. For liquids and pastes, it is sufficient to put a drop on a crystal and start the measurement. With modern small atr crystals and robust pressure clamps good sample contact can be obtained even for samples such as elastomers, fine powders, glass fibers reinforced polymers or minerals. Available crystal materials include diamond, zinc selenide and germanium.

ZnSe is an inexpensive material, it is suitable for the analysis of liquids and soft samples. However, ZnSe is prone to scratches and can only be used between pH 5-9.

Germanium has high refractive index and is used to study highly absorbing samples like carbon – black coloured rubbers. If high surface sensitivity is required like for thin layers, germanium is ideal due to low penetration depth. Diamond is very robust and chemically inert making it an ideal crystal material for routine measurements on a wide range of samples. Although the initial investment is higher, the cost over the instrument lifetime are often lower due to high resistance of diamond to scratches and its complete insolubility. The procedure of an ATR

measurement is straightforward, the steps are listed below:

- Cleaning the crystal (e.g. with cellulose tissue or isopropanol)
- Measuring the background with atr unit
- Placing the sample on the crystal ensuring good contact
- Measuring the sample

ADVANTAGES OF ATR

- Faster sampling techniques
- Excellent sample to sample reproducibility
- Minimal operator induced variations

In order to achieve a high quality spectrum some requirements must be fulfilled . they are as follows:

- Good contact between sample and ATR crystal has to be ensured as evanescent wave penetrates only upto a specific number of microns onto the sample
- The refractive index of crystal must be significantly higher than that of sample. since the typical refractive indices for ATR crystal are between 2- 4 and typical values for organic substances such as polymer range from ca. 1.2 – 1.5 , a large number of ir-active samples can be measured.[12]

I.R Absorbance vibrational spectroscopy

When a sample matter, for instance a pure molecule, is placed in the path of an IR beam light between the source and the detector, the

molecule will absorb only the frequency of mid-IR that coincides with the frequency of the vibration allowing the molecule enters in a resonant vibration status. IR absorbance spectroscopy extensively treated in [13 -15] measures the loss of IR radiation transmitted through a sample across an interval of frequencies of electromagnetic spectrum. Depending on the selected interval of wavelengths, near-IR spectroscopy, mid -IR spectroscopy, and far-IR spectroscopy (THz spectroscopy) can be performed using near-IR radiation, mid-IR radiation, and far-IR radiation, respectively. Mid-IR absorbance spectroscopy plots the recorded intensity of absorption bands versus an interval of wavenumbers, , from 4000 to 400 cm^{-1} , which corresponds to changes of vibrational energy levels from the ground level to the first energy level ($E_0 \rightarrow E_1$) in molecules.

Fundamental vibrational modes (also called normal modes) that are detectable by mid-IR spectroscopy are mainly represented by bond stretching (either symmetric, ν_s , and antisymmetric, ν_{as}) and bond deformations (mainly symmetric and antisymmetric bending, δ_s and δ_{as} respectively; other vibrational modes are twisting, γ_t , wagging, γ_w , rocking, γ_r , and scissoring motions. Fundamental vibrations concerning with water molecule are shown in **Figure 1c**. In a free H–O–H molecule the antisymmetric and symmetric stretching

vibrations (ν_{as} and ν_{s} , respectively) and the bending (δ) deformations of O–H group occur at $\sim 3500\text{ cm}^{-1}$, $\sim 1650\text{ cm}^{-1}$, and $\sim 600\text{ cm}^{-1}$, respectively. Since the frequency of a vibration is concurrently determined by the bond strength, the vibrational mode and the reduced mass, m_r , of atoms composing chemical groups, the frequencies at which specific vibrations occur within the spectrum are fairly constant for a given functional group (e.g., $-\text{CH}_2$, $-\text{C}=\text{O}$, O–H, etc.), as summarized in Table 1. For instance, the stretch of methylene group, ($\nu_{as}\text{ CH}_2$ and $\nu_{s}\text{ CH}_2$), in molecules occur between $\sim 2950\text{ cm}^{-1}$ and $\sim 2860\text{ cm}^{-1}$, respectively. As indicated in the harmonic oscillator model of (**Figure 1**), each of the two atoms (or groups) connected by the bond has an associated charge. If the two atoms are identical (e.g. O_2 , N_2 , etc.) and only one fundamental vibration can occur, e.g. ν_{s} , there will be no net change of dipole moment during the vibrational transition and therefore there will be no detectable mid-IR activity. Therefore, also net change in the dipole moment must occur in the group molecule in order for a particular vibrational mode to be detectable by mid-IR spectroscopy. For instance, the planar CO_2 molecule has no permanent dipole moment, since the individual bond dipoles exactly cancel each other during symmetric stretching vibration ($\nu_{s}\text{ O}-\text{C}-\text{O}$) occurring at $\sim 1480\text{ cm}^{-1}$. Nevertheless, the antisymmetric stretching, $\nu_{as}\text{ O}-\text{C}-\text{O}$ at

$\sim 2560\text{ cm}^{-1}$ and the bending vibrations $\delta\text{ O}-\text{C}-\text{O}$ at $\sim 500\text{ cm}^{-1}$, respectively can be detected because there is a net change in the dipole moment of CO_2 molecule at those wavenumbers allowing this molecule becomes detectable by mid-IR radiation. Moreover, also the magnitude of the dipole moment change determines the intensity of absorption band. For instance, whereas the $\nu_{\text{C}=\text{O}}$ bands have strong absorbance values more symmetric vibrations such as $\nu_{\text{C}=\text{C}}$ have weaker absorbance values or even they are not absorbing.

A tri atomic, angular molecule like H_2O produces 3 normal vibration modes: one symmetrical, one asymmetric stretching vibration and a bending vibration (**Figure 2**). In general, a polyatomic nonlinear molecule with N atoms has $3N-6$ distinct vibrations (six results from three translational and three rotational movements of the whole molecule, respectively). In linear molecules such as CO_2 , the number of possible vibrations is $3N-5$ (4 vibrational modes for CO_2). For human albumin, a protein of 609 amino acids with > 9000 atoms, the number of possible vibrations results > 27000 if we assume an average of 15 atoms per amino acid. Stretching vibrations of O_2 and N_2 as well as of many other non-IR active modes can be detected by Raman spectroscopy. Its principle of functioning is based on the selective inelastic scattering of a photon induced when a monochromatic radiation (any

excitation laser wavelength can be used) interacts with molecules that change their polarizability. A small fraction of light is scattered by an excitation associated with vibrational and rotational transitions of the molecule. The associated emerging photons of lower or of higher energy (frequency) can generate Stokes and anti-Stokes lines that in the Raman spectrum become detectable as shifts of frequency (Raman shifts) with respect to the incident radiation. Also this complementary spectroscopic technique, that will be not described longer in this review, has many potential application in cancer research and diagnosis.[16 -18]

IR vibrational spectroscopy and microscopy

All modern IR spectrometers use Fourier transform (FT) and are composed of the following common elements: an internal IR light source, the interferometer (basically a Michelson interferometer), and a single element detector connected with an amplifier and a computer .[13] The internal IR light is generated by a broadband, polychromatic continuum, conventional thermal light source such as a heated siliconcarbide rod (Globalar). Destructive or constructive interferences between IR light and matter are generated in the interferometer which consists of a system of mirrors, a stationary mirror and a moving mirror, and a semireflective lens (the beamsplitter, usually made of KBr). These interferences are recorded by the detector as a

sinusoidal variation of intensity (cosine function) to the optical retardation which is Fourier transformed (FT) to a spectrum (intensity as function wavenumbers. For a monochromatic radiation this results in a single line (band). With a broadband source (polychromatic, continuum source), constructive and destructive interferences in the spectral domain transmitted to and recorded by the detector will generate an interferogram. This represents the summation of all the cosine functions of all the individual wavelengths present in the source and zero path difference (ZPD) positions where all interferences will be in phase (the centre-burst). The application of mathematical function Fourier transform will convert this interferogram into a mid-IR single-beam spectrum where the number of peaks will reflect the number of detectable components in the sample. The intensity in peaks, reflecting the amount of different molecular bonds absorbing in specific regions of the IR spectrum, will be in relation with the relative abundance of different sample constituents. The minimum wavenumber difference that can be distinguished between two lines in a spectrum corresponds to spectral resolution.[14] FTIR absorbance spectroscopy without a microscope has absent or very limited spatial resolution.[19] and the sample spectrum limits to reflect the average biochemical and structural information referred to the whole probed sample. The addition of an FT-IR

microscope to the IR spectrometer has realized the possibility to detect vibrational motions of molecules within very restricted regions of the sample allowing the development of microFT-IR spectroscopy. The schematic layout of a typical microFT-IR apparatus is shown in Figure 2.

This apparatus is used to associate the optical image of selected object, for instance an individual cell, with the corresponding IR spectrum or its chemical image.

The FT-IR microscope is similar to visible light microscope but it does not employ glass refractive elements (glass is opaque to IR light of $\lambda > \sim 5\mu\text{m}$). For this reason microFT-IR performed in transmission (described in 3.1) requires that probing samples are deposited on optical windows (e.g. ZnSe, CaF₂, and BaF₂ crystals) that do not absorb, or absorb very low mid-IR radiation and have very high values of transmittance within a wide range of frequencies in the mid-IR region. Switching on the separate visible light source and associated optics, the IR microscope works like a standard optical microscope allowing the sample can be inspected by eyepiece. Several spot areas can be selected (and marked) moving the computerized precision XYZ sample stage. Digitalized images can be recorded by a Charged-Coupled Device (CCD) camera in order to associate the image of selected object visualized in the Liquid Crystal Display

(LCD) or on the computer screen with its corresponding FT-IR absorbance spectrum.

IR microscopes make use of Schwarzschild objectives (typically a combination of concave and convex mirrors aligned about the optical axis direct the beamlight through a hole) with a numerical aperture (NA) of ~ 0.61 . With the sample placed between the Schwarzschild objective and the condenser, the microscope works in the confocal configuration and generally a spatial resolution of $\sim \lambda/2$ is obtained. [20]

Adjustable aperture slits of IR opaque material (e.g. glass) allow to delimit selected spot areas from which IR signals will be acquired switching on IR light.

The FT-IR microscope is generally equipped with a single channel highly sensitive mercury cadmium telluride (MCT) photoconductive detector cooled in liquid nitrogen. Through connections with an amplifier the detector transmits the information to the computer. In a typical IR experiment the goal is to obtain reproducible spectra with an acceptable value of signal to noise ratio (S/N) as defined by the ratio of source power (SP) to the noise power (NP). To this scope, enough IR signal must be cumulated on the detector by performing a number of scans in continuous mode within the selected interval of wavenumbers (e.g. from 4000 cm⁻¹ to 600 cm⁻¹) at a selected scanner velocity (e.g 40 kHz). Reducing the aperture slits of microscope, the

flux of photons to the detector reduces as well as the value of S/N. Increasing the number of scans extends the acquisition time necessary to obtain each spectrum. In order to optimize the acquisition with a single element detector, the number of scans and the aperture sizes must be therefore balanced acting on the SP and/or on the NP terms of the following equation: $S/N = SP/NP$. Working with a conventional thermal source such as Globar, which emits mid-IR radiation in a 360 degrees distribution, and with aperture sizes reduced to $\sim 20\mu\text{m} \times 20\mu\text{m}$ or less, the photon throughput towards the detector significantly reduces while the detector noise remains constant and the value of S/N is strongly decreased independently on the duration of acquisition. Moreover, working with aperture sizes approaching the wavelength of mid-IR radiation ($2.5 \mu\text{m} - 25 \mu\text{m}$) the recorded spectra become increasingly distorted due to diffraction effects that give much more difficult the analyses in the spectra and results interpretation. Therefore, to increase S/N values one possibility is to modify the source power, SP, that is to increase the brightness or IR light, for instance using external IR light source from Synchrotron Radiation (SR). [21]

Whereas for aperture values $\geq 40\mu\text{m} \times 40\mu\text{m}$ there is no substantial advantage of using SR with respect to Globar, the highest brightness of SR IR source provides advantage over Globar for

shorter aperture settings ($\leq 20\mu\text{m} \times 20\mu\text{m}$ down to the diffraction limit of $\sim 3\mu\text{m} \times 3\mu\text{m}$). This is mainly due to the fact that the flux of SR IR photons is not a limiting factor during the acquisition of IR signals. In this situation, spatial resolution becomes diffraction limited.[22]

ATR DESIGN

Attenuated Total Reflectance (ATR) (Figure 4) is an internal reflection technique where the IR beam is directed through an internal reflection element (IRE) with higher refractive index, n_1 , to the sample with a lower refractive index, n_2 . The IRE element has the shape of a prism (or other geometric shape) and the crystal (ATR crystal) mounted in ATR objectives can be ZnSe or type IIA diamond ($n_1 = 2.4$), or Si ($n_1 = 3.42$), or Ge ($n_1 = 4$). This spectroscopic technique does not require a thin sample section is prepared and generates the mid-IR spectrum of the surface of probing sample placed into intimate contact with the IRE element of ATR objective and can be utilize also in experiments with wet samples such as living cells.[23]

Mid-IR radiation passing through the IRE will be totally internally reflected at the boundary separating the two media with $n_1 > n_2$ as well as it will provide an evanescent wave (decaying wave) that penetrates the surface of the sample with n_2 at an incident angle, i , that is greater than the critical angle, i_c . As a consequence, this evanescent wave will be attenuated by the mid-IR

absorption characteristic of the lower refractive index medium and will provide IR data about sample composition [24]. The depth of penetration, d_p , of evanescent wave has direct dependence on wavelength, λ , so that the depth of surface layer probed increases with increasing λ . A procedure called ATR correction [14] allows generating a spectrum in which the relative intensity of bands can be corrected allowing the ATR spectrum becomes very similar to an IR spectrum recorded in transmission. As for near-IR also mid-IR light can be coupled out of the spectrometer using silver halide (AgClBr) fiber optics that work as ATR elements [24]. Evanescent Wave Spectroscopy (EWS) is a new biophotonic technique based on the use of fiber optics in combination with IR spectroscopy. This very promising spectroscopic technique has many potential applications in preclinical and clinical cancer research and seems to realize the possibility to move IR spectroscopy and microscopy “from the bench to the bedside” [26, 27].

ANALYSIS IN THE SPECTRA

There are several different methods to approach the analysis of mid-IR spectra: from the simple inspection to identify the number of peaks to “chemometrics” where mathematical, statistical, and computer sciences methods are applied to improve the understanding of chemical information contained in typically broad and

complex IR spectroscopic data [28]. Patterns in the data can be identified, modeled and must undergo independent validation [29] to be applied in probabilistic neural networks [30] useful for pre-clinical and clinical trials. It is the availability of validated models obtained by interdisciplinary approaches that may represent the actual limitation for the application of microFT-IR spectroscopy in pre-clinical and clinical trials on cancer.

TRANSFLECTANCE

Transflectance (Figure 4) couples absorption and reflection through the sample [31]. It realizes when cells and tissues are lied on a glass slide coated with a thin layer of silver (low-e microscope slide) which makes the slide almost completely reflective to mid-IR radiation while it still remains totally transparent to visible light. Therefore, the sample can be inspected by visible light in transmission, whereas mid-IR radiation passes through the sample, is reflected back by the coating on the low-e slide and then passing through the sample again directs to the detector. The resulting mid-IR spectrum is closely equivalent to a mid-IR transmission spectrum recorded from a sample of double the section thickness. This convenient method to obtain representative spectra of individual cells can be strongly affected by severe distortions associated with resonant Mie scattering. Therefore, spectra necessitate to be always corrected for Mie

scattering before applying algorithms for the classification of spectra [32]. Principal advantages of transfection microFT-IR are that low-e microscope slides are inert and therefore suitable for cell culture, resist to high temperatures and therefore can be sterilized and reused, and are less costly than other biocompatible substrates such as CaF₂ and BaF₂.

APPLICATIONS OF ATR - FTIR

1. MONITORING OF DRUG RELEASE

- FTIR-ATR spectroscopic imaging has been used to study tablets containing diclofenac sodium and HPMC (hydroxypropyl methylcellulose) in different dissolution media which influence the solubility of diclofenac. The release profiles obtained by flow-through dissolution test suggest the presence of particles (or precipitates) in the dissolution medium. This is consistent with the results obtained by FTIR spectroscopy imaging, which indicated that the proposed techniques are superior to the ordinary dissolution test, when applied to poorly soluble drugs.[33]
- FTIR-ATR has been used for measuring the dissolution of Excedrin tablet composed from paracetamol and salicylic acid in its formulation. Dissolution is the accepted methodology for measuring the API release from the dosage forms. This approach was

found to be sensitive technique which can detect as low as 0.03 mg API/mL. FTIR spectra were subjected to baseline correction. For dissolution purposes, peak area at 1388 cm⁻¹ and at baseline of 1370 cm⁻¹ were used to calculate salicylic acid, meanwhile the absorption peak at 1246 cm⁻¹ and baseline at 1276 cm⁻¹ were selected for measuring paracetamol concentration.[34]

- FTIR-ATR was also used to simultaneously follow the diffusion of three drugs, namely cyanophenol, methyl nicotinate, and buthyl paraben as well as solvent across of silicone membrane. The diffusion of these drugs and the solvent was successfully explained with Fickian model. Using the absorbance changes at several frequencies and exploiting the penetration depth in ATR, the diffusion of these drugs can be predicted .[35]

2. QUALITATIVE ANALYSIS

- FTIR spectroscopy in combination with attenuated total reflectance (ATR) was used for the identification and quantification of ganciclovir polymorphs in pure three phases. Quantitative analysis of polymorphic mixtures is successfully carried out using partial least square (PLS) model. Each polymorph exhibits a characteristic FTIR spectra at fingerprint region (1800–600 cm⁻¹), with significant differences, in which each

polymorph can be readily identified. The R^2 obtained is > 0.98 . Fiber-optic near IR was also used for monitoring the polymorphisms of SaC, an anti-hypertension agent.[36]

- FTIR spectroscopy in combination with PLS using KBr pellet as sampling technique was used to quantify the amount of amorphous cyclosporine in crystalline cyclosporine .[37]

3. DETERMINATION OF ACTIVE PHARMACEUTICAL INGREDIENT

- One of the main advantages of FTIR spectroscopy for quantitative analyses of API is due to the possibility to simultaneously analyze some APIs using single spectral measurement[38]
- However, the co-existence of several APIs in pharmaceutical products meets several problems associated with the FTIR spectral overlapping. Fortunately today, some chemometrics techniques can overcome this problem without any separation step of sample components.[39]
- FTIR spectroscopy used for quantitative analysis of dimethicone in commercial tablets and capsules. Using absorbance measurement at $7.9 \mu\text{m}$, dimethicone has been successfully quantified with recovery percentage of 98-102 %. The developed method was linear over the concentration range of 20-50 mg/mL in

carbon tetrachloride. The United States Pharmacopeia (USP) also used this technique for quantitative analysis of simethicone.[40]

- FTIR-ATR was also proposed for direct determination of niflumic acid in the pharmaceutical gel with the aid of PLS calibration. The quantitative analysis was performed at frequency regions of $2300 - 1100 \text{ cm}^{-1}$. Using 14 factors, the coefficient of determination (R^2) for the relationship between actual and FTIR predicted values of niflumic acid is 0.9999, with root mean square error of prediction (RMSEP) of 0.2 %. The percentage of recovery obtained is in the range of 96.60 – 101.02 % .[41]
- FTIR spectroscopy used with attenuated total reflectance as sampling accessory for determination of sodium diclofenac in tablet. The quantification was performed with multivariate calibration of PLS. The combined frequency regions of $1233.5-1615.9$ and $2801.9-2976.4 \text{ cm}^{-1}$ was exploited for such determination. Three standard release tablets and two sustained release tablets containing between 25 and 100 mg of sodium diclofenac were successfully determined with the recovery percentage of 99.1–101.3 %.[42]

REFERENCES

1. Ellis, D.I. and Goodacre, R. (2006) Metabolic fingerprinting in disease diagnosis: biomedical applications of infrared and Raman spectroscopy. *Analyst*, 131: 875–885
2. Choo-Smith, L.P., Maquelin, K., van Vreeswijk, T., Bruining, H.A., Puppels, G.J., Ngo Thi, N.A., Kirschner, C., Naumann, D., Ami, D., Villa, A.M., Orsini, F., Doglia, S.M., Lamfarraj, H., Sockalingum, G.D., Manfait, M., Allouch, P., and Endtz, H.P. (2001) Investigating microbial (micro)colony heterogeneity by vibrational spectroscopy. *Applied Environmental Microbiology*, 67 (4): 1461–1469.
3. Kidder, L.H., Colarusso, P., Stewart, S.A., Levin, I.W., Appel, N.M., Lester, D.S., Pentchev, P.G., and Lewis, E.N. (1999) Infrared spectroscopic imaging of the biochemical modifications induced in the cerebellum of the Niemann–Pick type C mouse. *Journal of Biomedical Optics*, 4 (1): 7–13.
4. Kang, G.S., Ko, H.J., and Choi, C.K. (2003) Chemical bond structure of a-C:F films with a low dielectric constant deposited by using CH₄/CF₄ ICPCVD. *Journal of the Korean Physical Society*, 42 (5): 676–681.
5. Hofman, M., Pasieczna, S., Wachowski, L., and Ryczkowski, J. (2006) Speciation of functional groups formed on the surface of carbonaceous materials modified by NO. *Journal of Physics IV France*, 137: 287–290.
6. Skoog, Holler & Nieman, *Principles of instrumental analysis*, 5th Edn, Saunders College Publishing, USA: 184, (1998).
7. Robert D. Braun, *Introduction to Instrumental Analysis, Infrared Spectroscopy*, Pharma Book Syndicate, Hyderabad: 371-73, (2006).
8. Blanco, M. and Peguero, A. 2010. Analysis of pharmaceuticals by NIR spectroscopy without a reference method. *Trends Anal. Chem.* 29: 1127-1136.
9. Roggo, Y., Chalus, P., Maurer, L., LemaMartinez, C., Edmond, A. and Jent, N. 2007. A Review of near infrared spectroscopy and chemometrics in pharmaceutical technologies. *J. Pham. Biomed Anal.* 44: 683 – 700.
10. Massart, D.L. and Buydens, L. 1988. Chemometrics in pharmaceutical analysis. *J. Pham. Biomed. Anal.* 6: 535 – 545.
11. www.perkinelmer.com
12. www.azom.com, attenuated total reflection (ATR) mode- advantages of FTIR spectroscopy.
13. Chalmers JM, Griffiths PR. *Handbook of vibrational spectroscopy*. New York: J. Wiley, 2002
14. Griffiths PR, De Haseth JA. *Fourier transform infrared spectrometry*. Hoboken, NJ: WileyInterscience, 2007.

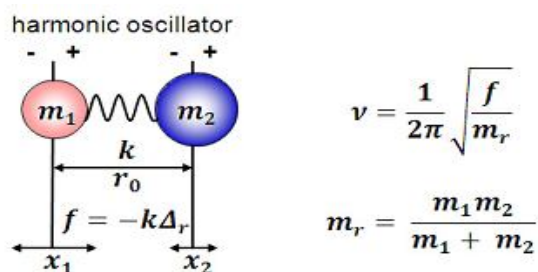
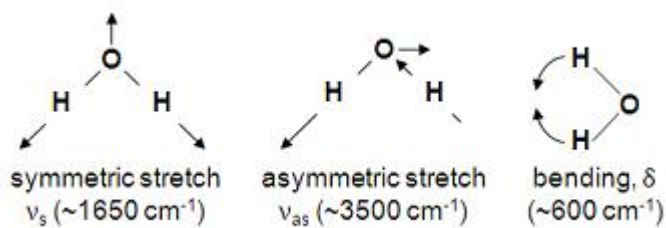
15. Diem M, Chalmers JM and Griffiths PR. Vibrational spectroscopy for medical diagnosis. Chichester, England ; Hoboken, NJ: John Wiley & Sons, 2008.
16. Zhang Y, Hong H and Cai W. Imaging with Raman spectroscopy. *Curr Pharm Biotechnol* 2010; 11: 654-661
17. Swain RJ, Stevens MM. Raman microspectroscopy for non-invasive biochemical analysis of single cells. *Biochem Soc Trans* 2007; 35: 544-549.
18. Barr H, Kendall C, Hutchings J, BazantHegemark F, Shepherd N and Stone N. Rapid endoscopic identification and destruction of degenerating Barrett's mucosal neoplasia. *Surgeon* 2011; 9: 119-123.
19. Lasch P, Naumann D. Spatial resolution in infrared microspectroscopic imaging of tissues. *Biochim Biophys Acta* 2006; 1758: 814-829
20. Carr GL. Resolution limits for infrared microspectroscopy explored with synchrotron radiation. *Review of Scientific Instruments* 2001; 72: 1613-1619.
21. Dumas P, Sockalingum GD and Sule-Suso J. Adding synchrotron radiation to infrared microspectroscopy: what's new in biomedical applications? *Trends Biotechnol* 2007; 25: 40-44.
22. Miller LM and Dumas P. Chemical imaging of biological tissue with synchrotron infrared light. *Biochim Biophys Acta* 2006; 1758: 846857.
23. Holman HYN, Bechtel HA, Hao Z and Martin MC. Synchrotron IR Spectromicroscopy: Chemistry of Living Cells. *Analytical Chemistry* 2010; 82: 8757-8765.
24. Bogomolny E, Huleihel M, Salman A, Zwielly A, Moreh R and Mordechai S. Attenuated total reflectance spectroscopy: a promising technique for early detection of premalignancy. *Analyst* 2010; 135: 1934-1940.
25. Raichlin Y, Fel L and Katzir A. Evanescentwave infrared spectroscopy with flattened fibers as sensing elements. *Opt Lett* 2003; 28: 2297-2299.
26. Sahu RK, Mordechai S. Spectral signatures of colonic malignancies in the mid-infrared region: from basic research to clinical applicability. *Future Oncol* 2010; 6: 1653-1667.
27. Mackanos MA, Contag CH. Fiber-optic probes enable cancer detection with FTIR spectroscopy. *Trends Biotechnol* 2010; 28: 317-323.
28. Lavine B, Workman J. Chemometrics. *Anal Chem* 2010; 82: 4699-4711.
29. Lasch P, Diem M, Hansch W and Naumann D. Artificial neural networks as supervised techniques for FT-IR microspectroscopic imaging. *J Chemom* 2007; 20: 209-220.

30. Podshyvalov A, Sahu RK, Mark S, Kantarovich K, Guterman H, Goldstein J, Jagannathan R, Argov S and Mordechai S. Distinction of cervical cancer biopsies by use of infrared microspectroscopy and probabilistic neural networks. *Appl Opt* 2005; 44: 3725-3734.
31. Lee J, Gazi E, Dwyer J, Brown MD, Clarke NW, Nicholson JM and Gardner P. Optical artefacts in transflection mode FTIR microspectroscopic images of single cells on a biological support: the effect of back-scattering into collection optics. *Analyst* 2007; 132: 750-755.
32. Harvey TJ, Gazi E, Henderson A, Snook RD, Clarke NW, Brown M and Gardner P. Factors influencing the discrimination and classification of prostate cancer cell lines by FTIR microspectroscopy. *Analyst* 2009; 134: 10831091.
33. Der Weerd, J.V. and Kazarian, S.G. 2005. Release of poorly soluble drugs from HPMC tablets studied by FTIR imaging and flow-through dissolution tests. *J. Pharm. Sci.* 94: 2096-2109.
34. Kassis, A., Bhawtankar, V.M. and Sowa Jr, J.R. 2010. Attenuated total reflection infrared spectroscopy (ATR-IR) as in situ technique for dissolution studies. *J. Pharm. Biomed. Anal.* 53: 269-273.
35. McAuley, W.J., Mader, K.T., Tetteh, J., Lane, M.E., Hadgraft, J. 2009. Simultaneous monitoring of drug and solvent diffusion across a model membrane using ATRFTIR spectroscopy. *Eur. J. Pharm. Sci.* 38: 378 – 383.
36. Salari, A. and Young, R.E. 1998. Application of attenuated total reflectance FTIR spectroscopy to the analysis of mixtures of pharmaceutical polymorphs. *Int. J. Pharm.* 163: 157-166.
37. Bertacche, V., Pini, E., Stradi, R., and Stratta, F. 2006. Quantitative determination of amorphous cyclosporine in crystalline cyclosporine samples by Fourier transform infrared spectroscopy. *J. Pharm. Sci.* 96(1): 159 – 166.
38. Moros, J., Garrigues, S., de la Guardia, M. 2010. Vibrational spectroscopy provides a green tool for multi-component analysis. *Trends Anal. Chem.* 29: 578 – 591.
39. Gallardo-Velázquez, T., Osorio-Revilla, G., Zuñiga-de Loa, M. and Rivera-Espinoza, Y. 2009. Application of FTIR-HATR spectroscopy and multivariate analysis to the quantification of adulterants in Mexican honeys. *Food Res. Int.* 42: 313– 318.
40. Torrado, G., Garcia-Arieta, A., de los Rios, F., Menendez, J.C., and Torrado, S. 1999. Quantitative determination of dimethicone in commercial tablets and capsules by Fourier

- transform infrared spectroscopy. *J. Pham. Biomed Anal.* 19, 285 – 291.
41. Boyer, C., Bregere, B., Crouchet, S., Gaudin, K., and Dubost, J.P. 2006. Direct determination of niflumic acid in a pharmaceutical gel by ATR/FTIR spectroscopy and PLS calibration. *J. Pham. Biomed Anal.* 40: 433 – 437.
42. Mazurek, S. and Szostak, R. 2011. Comparison of infrared attenuated total reflection and Raman spectroscopy in the quantitative analysis of diclofenac sodium in tablets. *Vib. Spectros.* 57: 157–162.

Table 1. Properties of material

Material	Spectral region	Refractive index	Depth of penetration	of Hardness (Knoop)
ZnSe	20000-500	2.43	1.66	130
ZnS	22000-750	2.25	1.54	355
Ge	5000-600	4.01	0.65	550
Si	10000-100	3.42	0.81	11150
Diamond	45000-10	2.40	1.66	9000

**Figure 1:** The basis of infrared (IR) vibrational absorbance spectroscopy .
(The classical harmonic oscillator model)**Figure 2:** Fundamental vibrational modes of a molecule of free water detectable at specific frequency values within the mid-IR region of the electromagnetic spectrum.

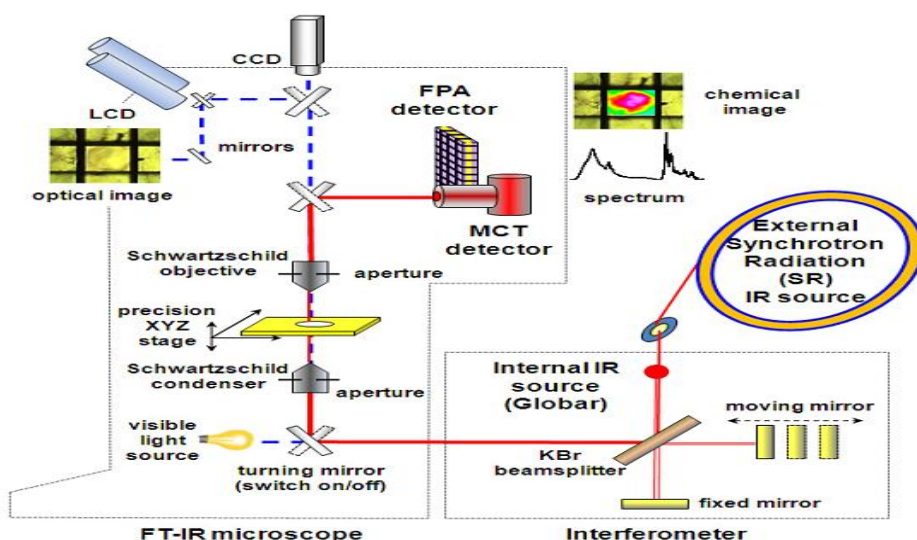


Figure 3: The schematic layout of components in an microFT-IR apparatus. The external IR beam is generally provided by Synchrotron Radiation and a dedicated beamline is required to extract IR light from the storage ring of a Synchrotron and to collimate IR light to the experimental area where the microFT-IR apparatus is usually located several meters from the exit port. The description of microFT-IR apparatus and the functioning of single components are in the text.

ATTENUATED TOTAL REFLECTANCE (ATR)

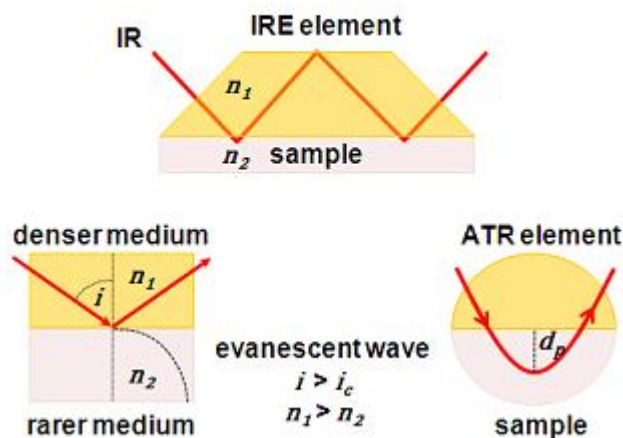


Figure 4: Attenuated Total Reflectance (ATR) technique

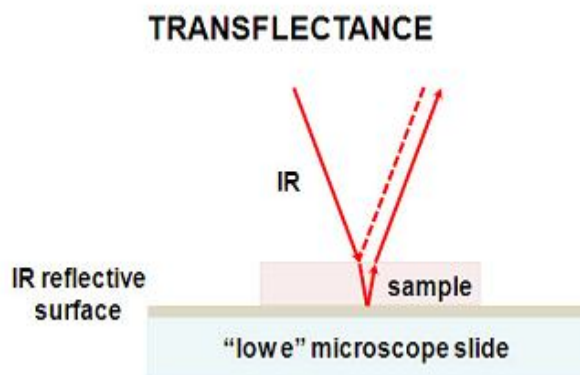


Figure 5: Transflectance